Non-Fickian diffusion enhanced by temperature

J.A. Ferreira[(1)], E. Gudiño[(2)] M. Grassi[(3)], P. de Oliveira[(1)]

(1) University of Coimbra, CMUC, Department of Mathematics, Coimbra, Portugal

(2) Department of Mathematics, Universidade Federal do Paraná, Brazil

(3) Department of Chemical Engineering, University of Trieste, Italy

ferreira@mat.uc.pt , egudino@ufpr.br , mario.grassi@dia.units.it ,poliveir@mat.uc.pt

July 27, 2023

Abstract

In this paper we present a novel mathematical model to describe the permeation of a fluid through a polymeric matrix, loaded with drug molecules, followed by its subsequent desorption. Both phenomena are enhanced by temperature. We deduce energy estimates and stability estimates for the weak solution of the model, showing that this solution of the problem is stable in bounded time intervals. Numerical simulations illustrate how the coupling effects, of viscoelastic properties and thermal external assistance, can have a central role in the design of drug delivery devices.

Keywords: Thermosensitive polymers, drug delivery, non-Fickian diffusion

1 Introduction

Over the past few years, the therapeutic effects resulting from Controlled Drug Delivery Devices (CDD) have clearly outperform the effects from Conventional Drug Delivery Devices (DD). Advances in material science and bionanotechnology have helped in the development of more efficient CDD, improving targeted release and decreasing undesirable side effects, largely attributable to the nonspecific bio-distribution and uncontrollable characteristics of DD [1].

Notably, CDD can provide targeted delivery for specific organs/tissues reducing both dosage frequency and drug toxicity. Even more, they can maintain proper drug rates in situ, leading to more effective therapeutic treatment. In cancer therapeutics, the targeted delivery can substantially reduce the side effects of chemotherapy. As a result, there is a steep rise in the development and study of CDD for targeted delivery in oncologic diseases [2].

Stimuli-responsive biomaterials (polymers, lipids and inorganic materials) have been used extensively as drug carriers nanoplatforms [3, 4]. They prevent drug extravasation into healthy tissues, they prolong blood circulation time and they improve drug accumulation while enhancing bioavailability at the target site [5]. These stimuli-responsive nanoplatforms are used for enhanced drug delivery triggered by endogenous and/or exogenous stimulus. The endogenous triggers can be set off by pH variations, hormone level, enzyme concentration, small biomolecules, glucose or redox gradient. The exogenous triggers, include temperature, magnetic fields, ultrasounds, light, electric pulses and high energy radiation [1]. We note that although drug molecules themselves can be designed for enhanced targeted delivery, in this work we will focus only on the material properties of the nanocarriers.

In the present paper we are interested on drug delivery enhanced by temperature. Polymeric nanocarriers can be stimulated to enhance drug release in tumors [6]. Usually, the thermosensitive nanocarriers maintain a low rate of delivery around the physiological temperature of

37ºC, and increase the release rapidly when the temperature rises above 40º–45ºC. [1]. Thermosensitive Hydrogels possess the ability to swell upon temperature changes, allowing an enhanced delivery. Several applications take advantage of this feature. We mention without being exhaustive, local delivery of anticancer drugs, anti-inflammatory drugs and antibiotics, also injectable formulations of peptides, such as urease, interleukin-2, and lidocaine [7].

In [8], a model for drug delivery enhanced by temperature was proposed. The model consists of two coupled quasilinear diffusion equations to study the evolution of temperature and drug concentration. In [9], the delivery is enhanced by both temperature and an electric field.

To the best of our knowledge, none of the models available in the literature take into consideration the viscoelastic properties of the polymers used for the enhanced delivery. The main disadvantage of such simplification is that the microstructural relaxation of the medium, induced by the penetrant, is ignored. Our aim is to propose a novel mathematical model for drug delivery enhanced by temperature taking into consideration the non-Fickian behavior of the material.

From a mathematical point of view, we establish the stability of a non-Fickian model that couples the absorption of a fluid, in a polymeric platform loaded with solid drug molecules, and its subsequent release, in which the two phenomena are stimulated by temperature. From the point of view of controlled drug release, our focus is to answer the following two questions :(1) How can the viscoelastic properties of polymeric platforms change the fluid absorption and the drug molecules release profiles? (2) How does an external temperature can be used to control the two-coupled phenomena?

In Section 2 we deduce a novel model for non-Fickian sorption by a viscoelastic material enhanced by temperature. Theoretical results regarding energy estimates and stability are shown in Section 3. Then, in Section 4 we couple the model with drug delivery. In Section 5 we present numerical simulations that illustrate the qualitative behavior of the model. Finally in Section 6 some conclusions are drawn.

2 Non-Fickian diffusion

When fluid permeates a viscoelastic material it causes a deformation which induces a stress that interacts with the Brownian motion of the fluid molecules [10]. As a consequence, the transport cannot be properly described by Fick's law of diffusion. Therefore, a modified flux must be considered, resulting from the sum of a Fickian flux J_F and a non-Fickian flux J_{NF} [11, 12, 13]. The equation for non-Fickian diffusion can be defined as

$$\frac{\partial c_\ell}{\partial t} = -\nabla \cdot \left(J_F(c_\ell) + J_{NF}(\sigma)\right), \tag{1}$$

where c_ℓ denotes the concentration of the fluid. The Fickian and non-Fickian fluxes are defined, respectively, by

$$J_F(c_\ell) = -D(c_\ell)\nabla c_\ell, \qquad J_{NF} = -D_v(c_\ell)\nabla\sigma,$$

with $D(c_\ell)$ and $D_v(c_\ell)$ representing the Fickian and non-Fickian diffusion coefficients, respectively. The function σ stands for the stress associated to fluid uptake and exerted by the polymer.

Equation (1) has to be coupled with an evolution equation for the stress which introduces the strain ε as a third variable. Assuming that the strain causes a viscoelastic stress response opposite to the flux [14], we consider

$$\sigma = -\int_0^t K(t-s)\frac{\partial \varepsilon}{\partial s} ds.$$

where K is the relaxation modulus of a mechanistic model consisting of springs and dampers in parallel and/or in series. Due to its versatility, we will use the generalized Maxwell-Wiechert model (Figure 1).

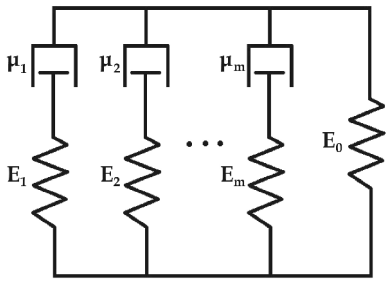

Figure 1: Generalized Maxwell-Wiechert model.

The model consists of $m+1$ arms in parallel, being the first m Maxwell fluid elements and the last one a free spring [15, Chapter 5]. The parameters E_i (for $i = 0, 1, \cdots, m$) denote the Young modulus of the spring elements, and the μ_i (for $i = 1, \cdots, m$) the viscosities of the dampers. It allows for an accurate representation of the behavior of a polymer, since the parameters can be fitted from experimental results.

In what follows we present an approach to introduce the influence of the temperature in the relaxation modulus associated to the generalized Maxwell-Wiechert model.

2.1 Temperature dependent Young modulus

Following the ideas from [14], we begin by assuming that we have a purely elastic material with initial Young modulus E^0, which represents the Young modulus of the sample at the reference temperature T_0. The cross-link density at the reference temperature of the sample can be defined as

$$\rho_x^0 = \frac{\xi^0}{V_0} \ , \tag{2}$$

where ξ^0 represents the number of moles of cross-links of the polymer at the reference temperature and V_0 the volume of the polymeric matrix at the reference temperature. In the swollen state the cross-link density becomes

$$\rho_x = \frac{\xi^0}{V_0 + V_0\beta(T - T_0)} \ , \tag{3}$$

where β is the volumetric temperature expansion coefficient, T is the temperature and T_0 is the reference temperature. Then, we obtain from (2) and (3) that

$$\frac{\rho_x}{\rho_x^0} = \frac{1}{1 + \beta(T - T_0)} \ . \tag{4}$$

As $\frac{\rho_x}{\rho_x^0} = \frac{E}{E^0}$ [14], we conclude from (4) that

$$E(T) = \frac{E^0}{1 + \beta(T - T_0)} \ .$$

The previous equation holds for purely elastic materials when $T \geq T_0$. In the case of viscoelastic materials we will assume that the elastic contributions in each Maxwell arm satisfy

$$E_k(T) = \begin{cases} \frac{E_k^0}{1+\beta(T-T_0)}, & T > T_0 \\ E_k^0, & T \leq T_0 \end{cases} \tag{5}$$

where E_k^0 for $k = 0, 1, 2, ..., m$ denotes the Young modulus of each spring element at the reference temperature.

We consider that the relaxation modulus can be defined as

$$\mathbb{E}(T(t), s, t) = E_0(T(t)) + \sum_{k=1}^{m} E_k(T(t)) e^{-\frac{1}{\mu_k}\int_s^t E_k(T(r))dr}.$$

The total stress is defined as,

$$\sigma(T(t), \varepsilon, t) = -\int_0^t \mathbb{E}(T(t), s, t)\frac{\partial \varepsilon}{\partial s} ds.$$

The relation between deformation and local solvent concentration can be nonlinear [14], however, to simplify our model we assume a linear relation between strain and the concentration of the penetrant c_ℓ. Therefore, we obtain after integrating by parts

$$\begin{aligned}\sigma(T(t), c_\ell(t), t) = &-\alpha \left(\sum_{k=0}^{m} E_k(T(t))\right) c_\ell(t) \\ &+ \alpha \sum_{k=1}^{m} \frac{E_k(T(t))}{\mu_k} \int_0^t E_k(T(s)) e^{-\frac{1}{\mu_k}\int_s^t E_k(T(r))dr} c_\ell(s) ds, \end{aligned} \tag{6}$$

where $\alpha > 0$ is the proportionality constant between the strain of the polymer and the concentration.

We note that (5) is a novel relation between the Young modulus and the temperature. There are several expression in the literature for different materials, however to the best of our knowledge, there is not a functional expression for viscoelastic materials that does not depend on fitting parameters.

2.2 Viscoelastic diffusion coefficient

Following ideas from [14, 16], we assume that the non-Fickian flux J_{NF} can be interpreted as a convective field. Considering that the polymeric sample is a porous media we obtain that

$$D_v(T(t), c_\ell(t)) = \Theta(T) c_\ell(t),$$

where $\Theta(T)$ is the temperature dependent permeability. It can be computed using the modified Kozeny-Carman equation [17, Ch 2.4.1]

$$\Theta(T) = \Theta_0 \left[\frac{1 - (1 - \phi_0) e^{f(T(t))}}{\phi_0}\right]^{3 - \frac{1}{m_0}} e^{-\frac{4}{3} f(T(t))},$$

where Θ_0 is the permeability at the reference temperature, m_0 is a fitting parameter, ϕ_0 the porosity at the reference temperature and

$$f(T(t) = p_1(T(t) - T_0) + \frac{p_2}{2}(T(t) - T_0)^2 + \frac{p_3}{3}(T(t) - T_0)^3 + \cdots,$$

where $p_1,\ p_2,\ p_3,\ \cdots$, are fitted from experimental data.

2.3 A non-Fickian model for fluid sorption enhanced by temperature

In what follows we couple the previous model for non-Fickian diffusion, with an evolution equation for the temperature T. Let us consider a polymeric sample $\Omega \in \mathbb{R}^3$ with boundary $\partial\Omega$.

In order to model the entrance of fluid in the polymeric matrix and the evolution of the stress we consider the equation

$$\frac{\partial c_\ell}{\partial t} = \nabla \cdot (D_\ell(T, cl)\nabla c_\ell + D_v(T, c_\ell)\nabla\sigma(T, c_\ell)) \qquad \text{in } \Omega \times (0, t_f], \tag{7}$$

where D_ℓ denotes the Fickian diffusion coefficient considering the Arrhenius equation and a Fujita type exponential dependence, defined here as

$$D_\ell(T, cl) = D_{0,\ell} e^{-\frac{E_A}{RT} - \beta_\ell(1 - \frac{c_\ell}{c_{eq}})},$$

where $D_{0,\ell}$ is the maximum diffusivity of the fluid, β_ℓ a dimensionless positive constant, E_A the activation energy for diffusion, R the universal gas constant and c_{eq} is defined by (11).

We couple (7) with the evolution of the temperature described by the equation

$$\frac{\partial T}{\partial t} = \nabla \cdot (D_T(T)\nabla T) + G(T) \qquad \text{in } \Omega \times (0, t_f], \tag{8}$$

where D_T is the thermal diffusivity and $G(T)$ stands for an external source.

We close system (7)-(8) with initial and boundary conditions

$$c_\ell(x, 0) = c_0 \qquad \text{for } x \in \Omega, \tag{9}$$

$$T(x, 0) = T_0 \qquad \text{for } x \in \Omega, \tag{10}$$

$$c_\ell(x, t) = c_{eq} \qquad \text{for } (x, t) \in \partial\Omega \times [0, t_f], \tag{11}$$

$$T(x, t) = T_{in} \qquad \text{for } (x, t) \in \partial\Omega \times [0, t_f]. \tag{12}$$

In what follows we study the stability of the initial-boundary value problem (7)-(12).

3 Theoretical results

3.1 Variational formulation

Let us consider the variational problem: Find $c_\ell \in L^2(0, t_f; H^1(\Omega))$, such that the boundary condition (11) and the initial condition (9) hold almost everywhere, described by

$$\begin{aligned}
&(\frac{\partial c_\ell}{\partial t}(t), v) + (D_\ell(T(t), c_\ell(t))\nabla c_\ell(t), \nabla v) = \\
&(\alpha D_v(T(t), c_\ell(t))\nabla \left(\left(\sum_{k=0}^{m} E_k(T(t)) \right) c_\ell(t) \right), \nabla v) \\
&- (\alpha D_v(T(t), c_\ell(t))\nabla \left(\sum_{k=1}^{m} \frac{E_k(T(t))}{\mu_k} \int_0^t E_k(T(s)) e^{-\frac{1}{\mu_k}\int_s^t E_k(T(r))dr} c_\ell(s) ds \right), \nabla v),
\end{aligned} \tag{13}$$

a. e. in $(0, t_f]$, for all $v \in H_0^1(\Omega)$.

For the temperature, we consider the following variational problem: Find $T \in L^2(0, t_f; H^1(\Omega))$, such that the boundary condition (12) and the initial condition (10) hold almost everywhere, described by

$$(\frac{\partial T}{\partial t}(t), v) + (D_T(T(t))\nabla T(t), \nabla v) = (G(T(t)), v), \tag{14}$$

a. e. in $(0, t_f]$, for all $v \in H_0^1(\Omega)$.

To simplify, in what follows we assume that the medium Ω is isotropic. Therefore, we replace it by $\Omega = (0, 1)$. In this case $\nabla v(x, t)$ is denoted by $\frac{\partial v}{\partial x}(x, t)$.

3.2 Energy estimates

In the analysis presented in this section we assume homogeneous Dirichlet boundary conditions for both T and c_ℓ.

An energy estimate for (14) was established in [8]. The result is presented in the next lemma. The following conditions are considered:

- β_1: $D_T \in \mathcal{C}_b^1(\mathbb{R})$ and $D_T \geq b_0 > 0$ in $\mathbb{R}$.
- β_2: $|G(y)| \leq b_1|y|$, for all $y \in \mathbb{R}$,

where $\mathcal{C}_b^m(\mathbb{R}^n)$ denotes the space of bounded functions with bounded m order partial derivatives in $\mathbb{R}^n$.

Lemma 1 ([8]). *Assume that conditions β_1 and β_2 are satisfied. If T is a solution of (14) such that $T \in \mathcal{C}^1(0, t_f; L^2(\Omega)) \bigcap L^2(0, t_f; H_0^1(\Omega))$, then*

$$\|T(t)\|^2 + \int_0^t \|\nabla T(s)\|^2 ds \leq \frac{e^{2b_1 t}}{\min\{1, 2b_0\}} \|T_0\|^2. \tag{15}$$

In order to deduce an energy estimate for the coupled system (13)-(14), we assume the conditions

- β_3: $D_\ell \in \mathcal{C}_b^1(\mathbb{R}^2)$ and $D_\ell \geq d_\ell > 0$ in $\mathbb{R}^2$.
- β_4: $D_v \in \mathcal{C}_b^1(\mathbb{R}^2)$ with $D_v \geq d_v$.

We note that the non-Fickian part of (7) cannot dominate the equation because it would lead to a total negative flux. Hence, we impose that

$$D_\ell(T(t), c_\ell(t)) - \alpha D_v(T(t), c_\ell(t)) \left(\sum_{k=0}^{m} E_k(T(t)) \right) \geq d_0 > 0, \quad \forall t \in [0, t_f], \tag{16}$$

where $d_0 \in \mathbb{R}$ is a positive constant.

We assume that $E_k(T(t))$, for each $k = 0, \cdots, m$, is replaced by a regularization of the form

$$\sum_{k=0}^{m} E_k(T(t)) \approx E(T(t)) = \sum_{k=0}^{m} \left(C_1 E_k^0 \arctan\left(C_2 - \beta\left(T(t) - T_0\right)\right) + C_3 \right),$$

where C_1, C_2 and C_3 are positive constants. For each $k = 0, \cdots, m$ we get that

$$\left| \left(C_1 E_k^0 \arctan\left(C_2 - \beta\left(T(t) - T_0\right)\right) + C_3 \right) \right| \leq C_{k,E},$$

for some positive constants $C_{k,E}$.

Furthermore, we suppose that the regularization satisfies the condition

- β_5: $\max\{|E|, |E'|, |E''|\} \leq C_E$ in $\mathbb{R}$.

To simplify the presentation we consider the notation

$$k_1(s,t) = \sum_{k=1}^{m} \frac{C_{k,E}^2}{\mu_k} e^{-\frac{1}{\mu_k}\int_s^t E_k(T(r))dr},$$
$$k_2(s,t) = \sum_{k=1}^{m} \frac{C_{k,E}^3}{\mu_k^2} e^{-\frac{1}{\mu_k}\int_s^t E_k(T(r))dr}.$$

Theorem 1. *Assume that conditions β_1-β_5 and (16) are satisfied. If c_ℓ is a solution of (13) and T is a solution of (14), such that*

$$c_\ell, T \in \mathcal{C}^1(0, t_f; L^2(\Omega)) \bigcap L^2(0, t_f; H_0^1(\Omega)),$$

then, there exists a positive constant θ, such that

$$\|c_\ell(t)\|^2 + \int_0^t e^{\theta \int_s^t F(r)dr} \|\nabla c_\ell(s)\|^2 ds \leq \|c_0\|^2 e^{\theta \int_0^t F(r)dr}, \tag{17}$$

provided that the non-Fickian diffusion-reaction equation (7) is diffusion dominated in the sense that

$$\hat{d}_0 = d_0 - \alpha d_v C_E \|\nabla(T(t) - T_0)\| > 0, \tag{18}$$

where

$$F(t) = 1 + \|\nabla T_0\|^2 + \|\nabla T(t)\|^2 + \int_0^t \|\nabla T(s)\|^2 ds.$$

Proof. Considering $v = c_\ell(t)$ in (13), we deduce

$$\begin{aligned} \frac{1}{2}\frac{d}{dt}\|c_\ell(t)\|^2 + d_0\|\nabla c_\ell(t)\|^2 \leq{}& \alpha d_v C_E \|\nabla(T(t) - T_0)\| \|\nabla c_\ell(t)\| \|c_\ell(t)\|_\infty \\ &+ \alpha d_v \|\nabla c_\ell(t)\| \int_0^t \|k_1(s,t)\|_\infty \|\nabla c_\ell(s)\| ds + \sum_{i-1}^{3} |P_i|, \end{aligned} \tag{19}$$

where

$$\begin{aligned} P_1 ={}& \alpha d_v \int_\Omega \nabla c_\ell(t) \sum_{k=1}^{m} \frac{E_k'(T(t))}{\mu_k} \nabla(T(t) - T_0) \int_0^t E_k(T(s)) J(s,t) c_\ell(s) ds \; dx, \\ P_2 ={}& \alpha d_v \int_\Omega \nabla c_\ell(t) \sum_{k=1}^{m} \frac{E_k(T(t))}{\mu_k} \int_0^t E_k'(T(s)) \nabla(T(s) - T_0) J(s,t) c_\ell(s) ds \; dx, \\ P_3 ={}& \alpha d_v \int_\Omega \nabla c_\ell(t) \sum_{k=1}^{m} \frac{E_k(T(t))}{\mu_k^2} \int_0^t E_k(T(s)) J(s,t) \left(\int_s^t E_k'(T(r)) \nabla(T(r) - T_0) dr \right) c_\ell(s) ds \; dx. \end{aligned}$$

considering the notation

$$J(s,t) = \exp\left(-\frac{1}{\mu_k} \int_s^t E_k(T(r)) dr \right).$$

As $\|c_\ell(t)\|_\infty \leq \|\nabla c_\ell(t)\|$, we replace (19) with

$$\begin{aligned} \frac{d}{dt}\|c_\ell(t)\|^2 + 2\hat{d}_0\|\nabla c_\ell(t)\|^2 \leq{}& 2\alpha d_v \|k_1\|_{L^2(0,t_f;L^\infty(\Omega))} \|\nabla c_\ell(t)\| \left(\int_0^t \|\nabla c_\ell(s)\|^2 \right)^{\frac{1}{2}} ds \\ &+ 2\sum_{i-1}^{3} |P_i|. \end{aligned} \tag{20}$$

For P_1, we have that

$$\begin{aligned} |P_1| &\leq \alpha d_v \beta \|k_1\|_{L^2(0,t_f;L^\infty(\Omega))} \| \left(\|\nabla T(t)\| + \|\nabla T_0\| \right) \|\nabla c_\ell(t)\| \left(\int_0^t \|c_\ell(s)\|_\infty^2 ds \right)^{\frac{1}{2}}, \\ &\leq \theta_1 \left(\|\nabla T_0\|^2 + \|\nabla T(t)\|^2 \right) \int_0^t \|\nabla c_\ell(s)\|^2 ds + \xi_1 \|\nabla c_\ell(t)\|^2, \end{aligned}$$

where $\xi_1 > 0$ is an arbitrary constant and

$$\theta_1 = \frac{1}{2\xi_1}\alpha^2 d_v^2 \beta^2 \|k_1\|^2_{L^2(0,t_f;L^\infty(\Omega))}.$$

Considering P_2, we deduce

$$\begin{aligned}|P_2| &\leq \alpha d_v \beta \|\nabla c_\ell(t)\| \int_0^t \|k_1(s,t)\|_\infty \|\nabla T(s) - \nabla T_0\| \|c_\ell(s)\| ds, \\ &\leq \left(\theta_2 \|\nabla T_0\|^2 + \theta_3 \int_0^t \|\nabla T(s)\|^2 ds\right) \int_0^t \|\nabla c_\ell(s)\|^2 ds + (\xi_2 + \xi_3)\|\nabla c_\ell(t)\|^2,\end{aligned}$$

where $\xi_2, \xi_3 > 0$ are arbitrary constants and

$$\theta_2 = \frac{1}{4\xi_2}\alpha^2 d_v^2 \beta^2 \|k_1\|^2_{L^2(0,t_f;L^\infty(\Omega))}, \qquad \theta_3 = \frac{1}{4\xi_3}\alpha^2 d_v^2 \beta^2 \left(\sum_{i=1}^m \frac{C_{k,E}^2}{\mu_k}\right)^2.$$

For P_3, we obtain that

$$\begin{aligned}|P_3| &\leq \alpha d_v \beta \|\nabla c_\ell(t)\| \int_0^t \|k_2(s,t)\|_\infty \left(\int_s^t \|\nabla T(r) - \nabla T_0\| dr\right) \|c_\ell(s)\|_\infty ds \\ &\leq \left(\theta_4 \|\nabla T_0\|^2 + \theta_5 \int_0^t \|\nabla T(s)\|^2 ds\right) \int_0^t \|\nabla c_\ell(s)\|^2 ds + (\xi_4 + \xi_5)\|\nabla c_\ell(t)\|^2,\end{aligned}$$

with $\xi_4, \xi_5 > 0$ arbitrary constants and

$$\theta_4 = \frac{1}{4\xi_4}\alpha^2 d_v^2 \beta^2 t_f^2 \|k_2\|^2_{L^2(0,t_f;L^\infty(\Omega))}, \qquad \theta_5 = \frac{1}{4\xi_5}\alpha^2 d_v^2 \beta^2 t_f \|k_2\|^2_{L^2(0,t_f;L^\infty(\Omega))}.$$

Using the estimates for $|P_i|$ in (20), we get that

$$\frac{d}{dt}\|c_\ell(t)\|^2 + 2\left(\hat{d}_0 - \sum_{i=1}^6 \xi_i\right)\|\nabla c_\ell(t)\|^2 \leq \ 2\theta_0 F(t) \int_0^t \|\nabla c_\ell(s)\|^2 ds, \tag{21}$$

where $\xi_6 > 0$ is an arbitrary constant and

$$\theta_0 = \max\{\frac{1}{4\xi_6}\alpha^2 d_v^2 \|k_1\|^2_{L^2(0,t_f;L^\infty(\Omega))}, \theta_1 + \theta_2 + \theta_4, \theta_1, \theta_3 + \theta_5\}.$$

Taking

$$\theta = \frac{2\theta_0}{\min\{1, 2\left(\hat{d}_0 - \sum_{i=1}^6 \xi_i\right)\}},$$

provided that the ξ_i are fixed by

$$\hat{d}_0 - \sum_{i=1}^6 \xi_i > 0,$$

when condition (18) is satisfied. From (21), we deduce

$$\frac{d}{dt}\left(\|c_\ell(t)\|^2 e^{-\theta \int_0^t F(r)dr} + \int_0^t e^{-\theta \int_0^s F(r)dr} \|\nabla c_\ell(t)\|^2\right) \leq 0.$$

Finally, after integration the result follows. □

3.3 Stability

A stability estimate for (14) was calculated in [8]. The result is presented in the next lemma.

Lemma 2 ([8]). *Assume that conditions β_1 and β_2 are satisfied. If T is a solution of* (14) *such that*

$$T \in \mathcal{C}^1(0, t_f; L^2(\Omega)) \bigcap L^2(0, t_f; H_0^1(\Omega) \bigcap W^{1,\infty}(\Omega)),$$

and $\tilde{T}$ is a perturbed solution of (14) *with respect to the initial data $\tilde{T}_0$, satisfying*

$$\tilde{T} \in \mathcal{C}^1(0, t_f; L^2(\Omega)) \bigcap L^2(0, t_f; H_0^1(\Omega)),$$

then, for $w_T = T - \tilde{T}$ there exists a positive constant ψ, such that

$$\|w_T(t)\|^2 + \int_0^t e^{\psi \int_s^t (1+\|\nabla T(r)\|_\infty) dr} \|\nabla w_T(s)\|^2 ds \leq \|w_{T_0}\|^2 e^{\psi \int_0^t (1+\|\nabla T(r)\|_\infty) dr}, \tag{22}$$

In what follows we consider a perturbation of the initial data c_0 and T_0. Then, we study the stability of the system with respect to the perturbed solutions $\tilde{c}_\ell$ and $\tilde{T}$ of (13) and (14), respectively.

Theorem 2. *Assume that conditions β_1-β_5,* (16) *and* (18) *are satisfied. If c_ℓ is a solution of* (13) *and T is a solution of* (14)*, such that*

$$c_\ell, T \in \mathcal{C}^1(0, t_f; L^2(\Omega)) \bigcap L^2(0, t_f; H_0^1(\Omega) \cap W^{1,\infty}(\Omega)),$$

and $\tilde{c}_\ell, \tilde{T}$ are two perturbed solutions, satisfying

$$\tilde{c}, \tilde{T} \in \mathcal{C}^1(0, t_f; L^2(\Omega)) \bigcap L^2(0, t_f; H_0^1(\Omega)).$$

Then, for $w_c = c_\ell - \tilde{c}_\ell$, there exist positive constants γ_1, γ_2 and γ_3 such that

$$\begin{aligned}
&\|w_c(t)\|^2 + \int_0^t e^{\gamma_1 \int_s^t G(r) dr} \|\nabla w_c(s)\|^2 ds \\
\leq &\|w_{c_0}\|^2 e^{\gamma_1 \int_0^t G(r) dr} + \gamma_3 \|w_{T_0}\|^2 \int_0^t e^{\gamma_1 \int_s^t G(r) dr} ds \\
&+ \gamma_2 \int_0^t e^{\gamma_1 \int_s^t G(r) dr} G(s) \left(\|w_T(s)\|_{H^1(\Omega)}^2 + \int_0^s \|w_T(r)\|_{H^1(\Omega)}^2 dr \right) ds,
\end{aligned} \tag{23}$$

with

$$\begin{aligned}
G(t) =& 1 + \|\nabla T(t) - \nabla T_0\|_\infty^2 + \|\nabla \tilde{T}(t) - \nabla \tilde{T}_0\|^2 + \|\nabla c_\ell(t)\|_\infty^2 \\
&+ \int_0^t \left(\|\nabla T(s) - \nabla T_0\|_\infty^2 + \|\nabla \tilde{T}(s) - \nabla \tilde{T}_0\|^2 + \|\nabla C(s)\|_\infty^2 \right) ds
\end{aligned}$$

provided that

$$\|\tilde{T}_0\| \leq \frac{d_\ell - \alpha d_v C_E}{\alpha d_v C_E}. \tag{24}$$

Proof. Considering $v = w_c(t)$ in (13) we obtain that

$$(\frac{\partial w_c}{\partial t}(t), w_c(t)) + (D_\ell(T(t), c_\ell(t)) \nabla c_\ell(t) - D_\ell(\hat{T}(t), \hat{c}_\ell(t)) \nabla \hat{c}_\ell(t), \nabla w_c(t)) = S_1 + S_2,$$

with

$$\begin{aligned}
S_1 =&(\alpha D_v(T(t),c_\ell(t))\nabla\left(\left(\sum_{k=0}^{m}E_k(T(t))\right)c_\ell(t)\right),\nabla w_c(t))\\
&-(\alpha D_v(\hat{T}(t),\hat{c}_\ell(t))\nabla\left(\left(\sum_{k=0}^{m}E_k(\hat{T}(t))\right)\hat{c}_\ell(t)\right),\nabla w_c(t)),\\
S_2 =&-(\alpha D_v(T(t),c_\ell(t))\nabla\left(\sum_{k=1}^{m}\frac{E_k(T(t))}{\mu_k}\int_0^t E_k(T(s))J(s,t)c_\ell(s)ds\right),\nabla w_c(t))\\
&+(\alpha D_v(\hat{T}(t),\hat{c}_\ell(t))\nabla\left(\sum_{k=1}^{m}\frac{E_k(\hat{T}(t))}{\mu_k}\int_0^t E_k(\hat{T}(s))\hat{J}(s,t)\hat{c}_\ell(s)ds\right),\nabla w_c(t)).
\end{aligned}$$

Summing and subtracting the term

$$(D_\ell(\hat{T}(t),\hat{c}_\ell(t))\nabla c_\ell(t),\nabla w_c(t)),$$

we deduce

$$\begin{aligned}
\frac{1}{2}\frac{d}{dt}\|w_c(t)\|^2+d_\ell\|\nabla w_c(t)\|^2\leq&\left|(\Big(D_\ell(T(t),c_\ell(t))-D_\ell(\hat{T}(t),\hat{c}_\ell(t))\Big)\nabla c_\ell(t),\nabla w_c(t))\right|\\
&+|S_1|+|S_2|
\end{aligned}\tag{25}$$

For the first term, we have that

$$\begin{aligned}
&\left|(\Big(D_\ell(T(t),c_\ell(t))-D_\ell(\hat{T}(t),\hat{c}_\ell(t))\Big)\nabla c_\ell(t),\nabla w_c(t))\right|\\
&\leq D_{x,\max}\|\nabla c_\ell(t)\|_\infty\|w_T(t)\|\|\nabla w_c(t)\|+D_{y,\max}\|\nabla c_\ell(t)\|_\infty\|w_c(t)\|\|\nabla w_c(t)\|\\
&\leq m_0\|\nabla c_\ell(t)\|_\infty^2\|w_T(t)\|^2+m_1\|\nabla c_\ell(t)\|_\infty^2\|w_c(t)\|^2+(\xi_1+\xi_2)\|\nabla w_c(t)\|^2,
\end{aligned}\tag{26}$$

where $\xi_1,\xi_2>0$ are arbitrary constants and

$$m_0=\frac{D_{x,\max}^2}{4\xi_1},\qquad m_1=\frac{D_{y,\max}^2}{4\xi_2}.$$

For S_1, we sum and subtract the terms

$$\begin{aligned}
&(\alpha D_v(\tilde{T}(t),\tilde{c}_\ell(t))\left(\sum_{k=0}^{m}E_k'(T(t))\right)\nabla(T(t)-T_0)c_\ell(t),\nabla w_c(t)),\\
&(\alpha D_v(\tilde{T}(t),\tilde{c}_\ell(t))\left(\sum_{k=0}^{m}E_k'(\tilde{T}(t))\right)\nabla(T(t)-T_0)c_\ell(t),\nabla w_c(t)),\\
&(\alpha D_v(\tilde{T}(t),\tilde{c}_\ell(t))\left(\sum_{k=0}^{m}E_k'(\tilde{T}(t))\right)\nabla(\tilde{T}(t)-\tilde{T}_0)c_\ell(t),\nabla w_c(t)),
\end{aligned}$$

to deduce

$$\begin{aligned}
|S_1|\leq&(m_2\|\nabla(T(t)-T_0)\|_\infty^2+m_3\|\nabla c_\ell(t)\|_\infty^2)\|w_T(t)\|^2\\
&(m_4\|\nabla(T(t)-T_0)\|_\infty^2+m_5\|\nabla c_\ell(t)\|_\infty^2)\|w_c(t)\|^2\\
&+m_6\|\nabla(w_T(t)-w_{T_0})\|^2\\
&+(\alpha d_vC_E+\alpha d_vC_E\|\nabla(\tilde{T}(t)-\tilde{T}_0)\|+\sum_{i=3}^{9}\xi_i)\|\nabla w_c(t)\|^2
\end{aligned}\tag{27}$$

with

$$
\begin{aligned}
m_2 &= \frac{1}{4\xi_3}\alpha^2 C_E^2 \|c_\ell\|^2_{L^\infty(0,t_f;L^\infty(\Omega))} D^2_{v,x,\max} + \frac{1}{4\xi_4}\alpha^2 d_v^2 C_E^2 \|c_\ell\|^2_{L^\infty(0,t_f;L^\infty(\Omega))},\\
m_3 &= \frac{1}{4\xi_5}\alpha^2 C_E^2 D^2_{v,x,\max} + \frac{1}{4\xi_6}\alpha^2 d_v^2 C_E^2,\\
m_4 &= \frac{1}{4\xi_7}\alpha^2 C_E^2 \|c_\ell\|^2_{L^\infty(0,t_f;L^\infty(\Omega))} D^2_{v,y,\max} + \frac{1}{4\xi_8}\alpha^2 d_v^2 C_E^2,\\
m_5 &= \frac{1}{4\xi_9}\alpha^2 C_E^2 D^2_{v,y,\max},\\
m_6 &= \frac{1}{4\xi_{10}}\alpha^2 d_v^2 C_E^2 \|c_\ell\|^2_{L^\infty(0,t_f;L^\infty(\Omega))},
\end{aligned}
$$

where the $\xi_i > 0$ are arbitrary constants for all $i = 3, \cdots, 9$.

Analogously for S_2, there exists positive constants $m_7, \cdots, m_{13}$, such that

$$
\begin{aligned}
&|S_2| \leq \\
&m_7 \left(\|\nabla(T(t) - T_0)\|^2_\infty + \int_0^t \|\nabla(T(s) - T_0)\|^2_\infty ds + \int_0^t \|\nabla c_\ell(s)\|^2_\infty ds \right) \|w_T(t)\|^2 \\
&+ m_8 \left(\|\nabla(T(t) - T_0)\|^2_\infty + m \int_0^t \|\nabla(T(s) - T_0)\|^2_\infty ds + \int_0^t \|\nabla c_\ell(s)\|^2_\infty ds \right) \|w_c(t)\|^2 \\
&+ m_9 \|\nabla(w_T(t) - w_{T_0})\|^2 + m_{10} \int_0^t \|\nabla(w_T(s) - w_{T_0})\|^2 ds \\
&+ m_{11} \left(\int_0^2 \|\nabla(T(s) - T_0)\|^2_\infty ds + \int_0^t \|\nabla c_\ell(s)\|^2_\infty ds \right) \int_0^t \|w_T(s)\|^2 ds \\
&+ m_{12} \left(\|\nabla(\tilde{T}(t) - \tilde{T}_0)\|^2 + \int_0^t \|\nabla(\tilde{T}(s) - \tilde{T}_0)\|^2 ds \right) \int_0^t \|\nabla w_T(s)\|^2 ds \\
&+ m_{13} \left(1 + \|\nabla(\tilde{T}(t) - \tilde{T}_0)\|^2 + \int_0^t \|\nabla(\tilde{T}(s) - \tilde{T}_0)\|^2 ds \right) \int_0^t \|\nabla w_c(s)\|^2 ds \\
&+ \xi_{11} \|\nabla w_c(t)\|^2,
\end{aligned} \tag{28}
$$

where $\xi_{11} > 0$ is an arbitrary constant.

Considering (26)-(28) in (25), we obtain that there exist positive constants γ_1, γ_2 and γ_3 such that

$$
\begin{aligned}
&\frac{d}{dt}\|w_c(t)\|^2 + \|\nabla w_c(t)\|^2 \\
&\leq \ \gamma_1 G(t) \left(\|w_c(t)\|^2 + \int_0^t \|\nabla w_c(s)\|^2 ds \right) + \gamma_3 \|w_{T_0}\|^2 \\
&\quad + \gamma_2 G(t) \left(\|w_T(t)\|^2 + \|\nabla w_T(t)\|^2 + \int_0^t \left(\|w_T(t)\|^2 + \|\nabla w_T(s)\|^2 \right) ds \right),
\end{aligned}
$$

provided that

$$
d_0 - \alpha d_v C_E \|\nabla(\tilde{T}(t) - \tilde{T}_0)\| > 0,
$$

which holds when condition (24) is satisfied.

We also consider that the arbitrary constants ξ_i are fixed by

$$
d_0 - \alpha d_v C_E \|\nabla(\tilde{T}(t) - \tilde{T}_0)\| - \sum_{i=1}^{11} \xi_i > 0.
$$

Finally, the result follows after multiplication by $e^{\int_0^t G(s)ds}$ and integration. □

We note that condition (24) means that the perturbation of the initial data for the temperature, is bounded by the set of physical parameters that guarantee that the total flux in (7) is positive.

4 Coupling with drug delivery

In order to consider the effect of geometry on drug nanocrystal water solubility, we assume the following thermodynamic model [18]:

$$C_s(T) = \frac{M_d X_d(T)}{M_s(1 - X_d(T))}\rho_{sol},$$

where M_d and M_s are, respectively, the drug and the solvent molecular weights, ρ_{sol} is the solvent density, C_s is the mass/volume nanocrystal solubility and X_d is the drug molecular solubility, defined by

$$X_d(T) = \frac{1}{\gamma_d}\left(\frac{T}{T_m}\right)^{\Delta c_p/R} \exp\left(-\left[\frac{\Delta h_m}{RT}\left(1 - \frac{T}{T_m}\right) + \frac{\Delta c_p}{R}\left(1 - \frac{T_m}{T}\right)\right]\right),$$

Δh_m and Δc_p are, respectively, the drug molar melting enthalpy and the difference between the solid-liquid drug molar specific heat at constant pressure, γ_d is the drug activity coefficient and T_m is the nanocrystal melting temperature.

In order to simplify the model, we assume that γ_d and ρ_{sol} do not change with temperature, thus, considering the ratio $C_s(T)/C_s(T_0)$ we get that

$$\begin{aligned}\frac{C_s(T)}{C_s(T_0)} =& \frac{X_d(T)(1 - X_d(T_0))}{X_d(T_0)(1 - X_d(T))} \\ =& \left(\frac{T}{T_0}\right)^{\Delta c_p/R} \exp\left(\frac{1}{R}\left(\frac{1}{T_0} - \frac{1}{T}\right)(\Delta h_m - \Delta c_p T_m)\right),\end{aligned}$$

Considering the solubility of the drug and the evolution of non-Fickian diffusion of the permeant fluid in the polymeric matrix, the concentration of dissolved and solid drug in the polymer are given by the following transport equations,

$$\begin{aligned}\frac{\partial c_d}{\partial t} =& \nabla \cdot (D_d(T, c_\ell)\nabla c_d + v(c_\ell)c_d)) \\ &+ K_d c_\ell \left(1 - \frac{c_d}{C_s(T)}\right) H(c_s) H\left(1 - \frac{c_d}{C_s(T)}\right) \qquad \text{in } \Omega \times (0, t_f], \qquad (29) \\ \frac{\partial c_s}{\partial t} =& -K_d c_\ell \left(1 - \frac{c_d}{C_s(T)}\right) H(c_s) H\left(1 - \frac{c_d}{C_s(T)}\right) \qquad \text{in } \Omega \times (0, t_f], \qquad (30)\end{aligned}$$

where c_d and c_s denote the concentrations of dissolved and solid drugs, respectively, K_d the constant dissolution rate of the drug and H represents the Heaviside function. We denote by D_d the Fickian diffusion coefficient of the drug defined by

$$D_d(T, cl) = D_{0,d} e^{-\frac{E_A}{RT} - \beta_d(1 - \frac{c_\ell}{c_{eq}})},$$

where $D_{0,d}$ is the maximum diffusivity of the drug and β_d a dimensionless positive constant. The stress field introduced in (7) is responsible for a convective solvent transport that, in turn, implies a convective drug transport of dissolved drug. Therefore we define the convective velocity as

$$v(c_\ell) = D_v(T, c_\ell)\frac{\nabla \sigma(T, c_\ell)}{c_\ell}$$

We note that we are assuming that drug dissolution can only occur in the presence of the incoming solvent, if the solid phase is present and if the concentration of dissolved drug is smaller than the solubility. That is, only when $c_\ell > 0$, $c_s > 0$ and $c_d < C_s$. In Figure 2 we show the behavior of the ratio $C_s(T)/C_s(T_0)$ as a function of the temperature, with $T(t) = 290 + t$ for $t \in [0, 320]$. The parameters for C_s are fixed by the reference values considered in Section 5. We can see that the solubility is an increasing function of T.

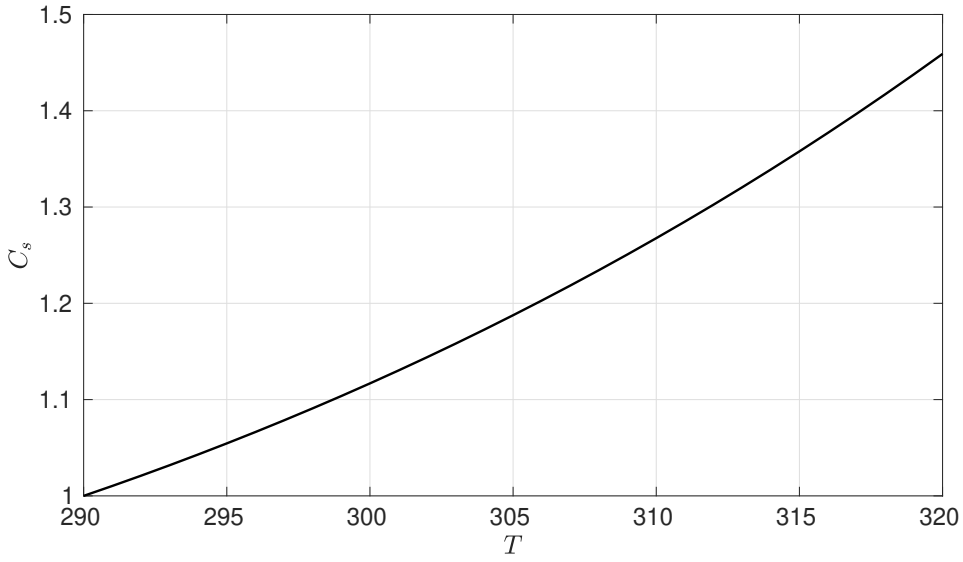

Figure 2: Solubility ratio $C_s(T)/C_s(T_0)$ with $T(t) = 290 + t$ for $t \in [0, 320]$.

The system (29)-(30) is closed with initial and boundary conditions:

$$c_d(x, 0) = 0 \qquad \text{for } x \in \Omega, \tag{31}$$

$$c_s(x, 0) = c_0 \qquad \text{for } x \in \Omega, \tag{32}$$

$$c_d(x, t) = 0 \qquad \text{for } x \in \partial\Omega \times [0, t_f]. \tag{33}$$

Thus, we are considering that the polymeric matrix has an initial loading of solid drug $c_0 \in \mathbb{R}$ and that all the dissolved drug that reaches the boundary is removed from the domain (perfect sink condition).

5 Numerical simulations

In this section we present some numerical simulations for the one dimensional case in $[0, L]$. In order to reduce the computational cost, we will consider symmetry conditions at the axis $x = 0$.

Let $h = (h_1, h_2 \cdots, h_N)$ be such that $\sum_{j=1}^{N} h_j = L$. Each vector h induces in the spatial domain $[0, L]$ a nonuniform grid $I_h = \{x_j,\ j = 0, 1, \cdots, N\}$, where $x_0 = 0$, $x_N = L$, and $x_j - x_{j-1} = h_j$, for all $j = 1, 2, \cdots, N$.

In the time domain $[0, t_f]$ we set a uniform grid $I_{\Delta t} = \{t_n,\ n = 0, 1, \cdots, M\}$, where $t_0 = 0$, $t_M = t_f$, and $t_n - t_{n-1} = \Delta t$, for all $n = 1, 2, \cdots, M$.

We denote by $\mathbb{W}_h$ the space of grid functions defined in I_h. By $\mathbb{W}_{h,0}$ we represent the subspace of $\mathbb{W}_h$ of functions null on the boundary points. By D_{-t} and D_{-x} we denote the usual backward finite difference operators in time and space, respectively.

In order to solve numerically (14), we propose the following implicit-explicit (IMEX) finite difference method

$$D_{-t}T_h^n(x_j) = D_x^{\frac{1}{2}}(D_T(M_hT_h^{n-1}(x_j))D_{-x}T_h^n(x_j)) + G(T_h^{n-1}(x_j)), \tag{34}$$

where

$$D_x^{\frac{1}{2}}u_h(x_j) = \frac{u_h(x_{j+1}) - u_h(x_j)}{h_{j+1/2}}, \quad h_{j+1/2} = \frac{h_{j+1} + h_j}{2},$$

and

$$M_hu_h(x_j) = \frac{u_h(x_{j-1}) + u_h(x_j)}{2},$$

for all $u_h \in I_h$.

To simplify the presentation we consider the notation

$$F_h(x_j, n, s) = \alpha \sum_{k=1}^{m} \frac{1}{\mu_k} E_k(M_hT_h^n(x_j))E_k(M_hT_h^s(x_j))e^{-\frac{1}{\mu_k}\Delta t \sum_{r=s}^{n-1} E_k(M_hT_h^r(x_j))}.$$

For the numerical solution of (13), we propose the following IMEX finite difference method

$$\begin{aligned} D_{-t}c_{\ell,h}^n(x_j) =& D_x^{\frac{1}{2}}(D_\ell(M_hT_h^n(x_j), M_hc_{\ell,h}^{n-1}(x_j))D_{-x}c_{\ell,h}^n(x_j)) \\ & - \alpha D_x^{\frac{1}{2}}\left(D_v(M_hT_h^n(x_j), M_hc_{\ell,h}^{n-1}(x_j))D_{-x}\left(\sum_{k=0}^{m} E_k(M_hT_h^n(x_j))c_{\ell,h}^n(x_j)\right)\right) \\ & + \Delta t \sum_{s=0}^{n-1} D_x^{\frac{1}{2}}(D_v(M_hT_h^n(x_j), M_hc_{\ell,h}^{n-1}(x_j))D_{-x}(F_h(x_j, n, s)c_{\ell,h}^s(x_j))). \end{aligned} \tag{35}$$

In Section 5.1, we include numerical simulations showing that the proposed schemes (34) and (35), are second order convergent in space and first order convergent in time.

In order to illustrate the qualitative behavior of the model we consider the following reference values taken from [8] [14], [16], [17] and [19]:

$L = 5e{-}3$ m, $t_f = 1000$ s, $D_T = 1e{-}8$ m^2/s, $G(T) = 0$, $T_0 = 290$ K, $T_{in} = 325$ K, $\beta = 80e{-}4$ 1/K, $E_0 = 9e3$ Pa, $E_1 = 2e3$ Pa, $\mu_1 = 2.25e4$ Pa·s, $\phi_0 = 50$, $m_0 = 1.5$, $E_A/R = 2.43e2$ K, $c_{eq} = 700$ kg/m^3, $D_{\ell,0} = 1e-8$ m^2/s, $\beta_\ell = 1.5$, $c_0 = 4.5$ kg/m^3, $D_{d,0}5e-8$ m^2/s, $\beta_d = 0.5$, $K_d = 1e{-}7$ s^{-1}, $C_s(T_0) = 0.02$ kg/m^3, $T_m = 494.05$ K, $\Delta c_p = 180.26$ J/(mol·K), $\Delta h_m = 43884.6$ J/mol, $\Delta t = 0.01$ s, $h = 1e-4$ m.

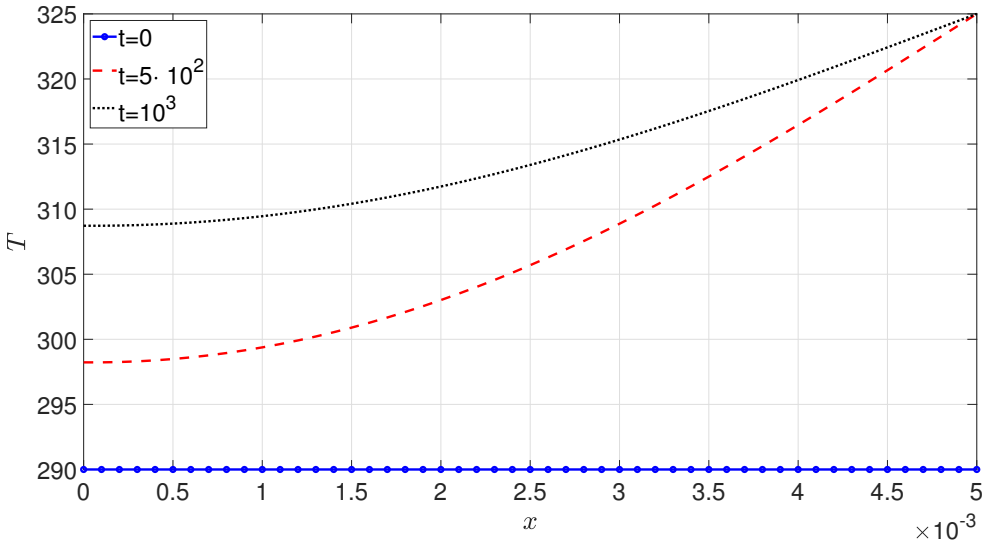

Figure 3: Temperature for $t = 0$, $t = 5 \cdot 10^2$ and $t = 10^3$ in $[0, L]$.

In Figure 3 we show the evolution of the temperature at different times. At $t = 0$ we observe that the initial constant temperature T_0 is evenly distributed in the spatial domain; then for $t = t_f/2$ and $t = t_f$ we observe an increase in the temperature as we are assuming that we have a constant source of temperature T_{in} at $x = L$.

In Figure 4 we plot the concentration c_ℓ as a function of x, for time points t_0, $t_f/2$ and t_f. The concentration inlet is located at $x = L$. Therefore, the concentration increases from right to left in the spatial domain as time increases.

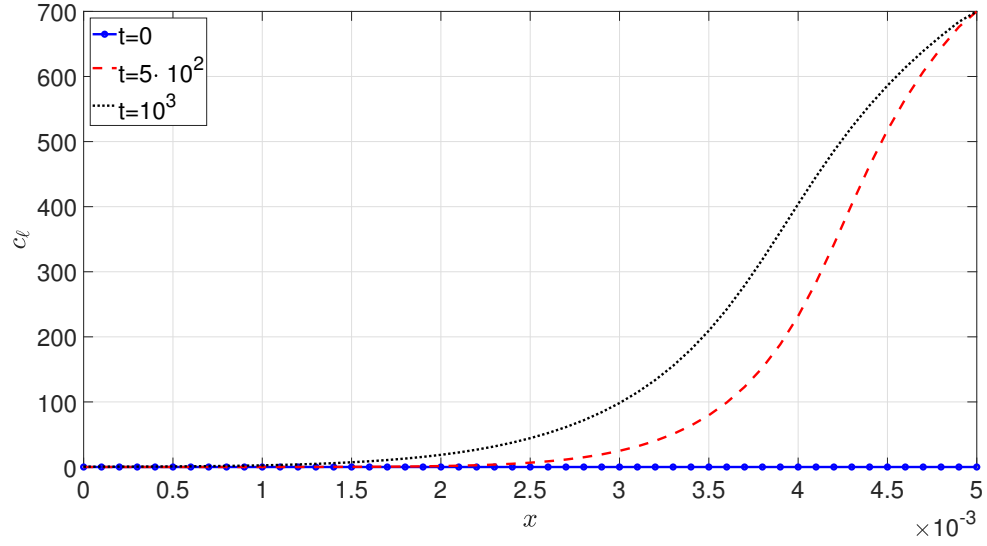

Figure 4: Concentration c_ℓ for $t = 0$, $t = 5 \cdot 10^2$ and $t = 10^3$ in $[0, L]$.

For $t = t_f$, we exhibit in Figure 5 a plot of the concentration of the fluid, as a function of x considering three different regimes: Fickian enhanced by temperature, non-Fickian and non-Fickian enhanced by temperature. The fastest absorption occurs for Fickian diffusion enhanced by temperature. When the relaxation of the polymer is included, in both non-Fickian diffusion regimes, diffusion of the permeating fluid slows down since there is an opposition to the flow

that decreases with respect to the temperature. Therefore, the slower absorption is observed in the non-Fickian regime with no temperature enhancement.

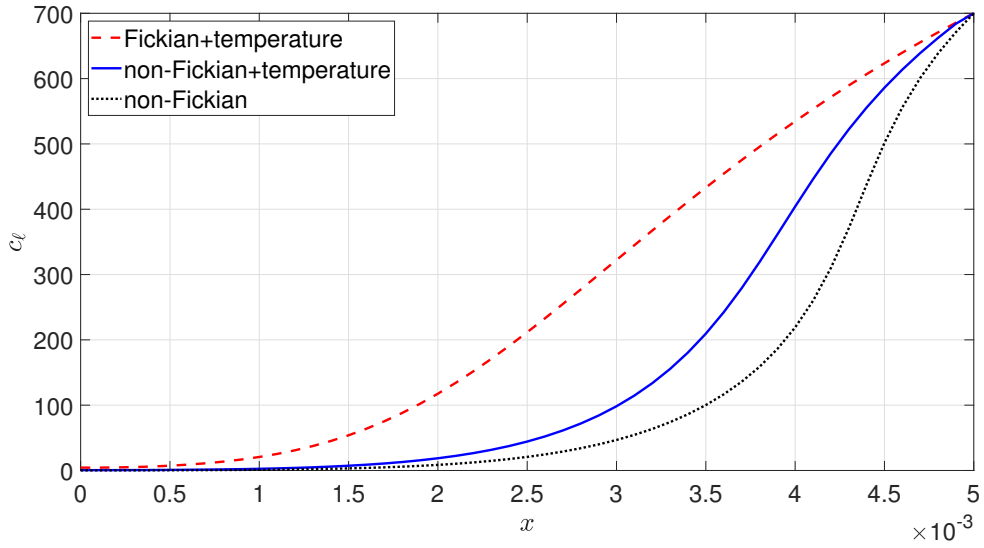

Figure 5: Concentration c_ℓ for $t = t_f$ in $[0, L]$.

We define the total mass M_i for $i = \ell, d, s$, as

$$M_i(t) = \int_0^L c_i(x,t)dx, \qquad \text{for } t \in [0, t_f].$$

The mass variation of c_ℓ is depicted in Figure 6. We observe a behavior consistent with the results in Figure 5. That is, less fluid mass is absorbed when non-Fickian diffusion with no temperature enhancement is considered and the highest accumulation is attained when the phenomenon is modeled with Fickian diffusion enhanced by temperature.

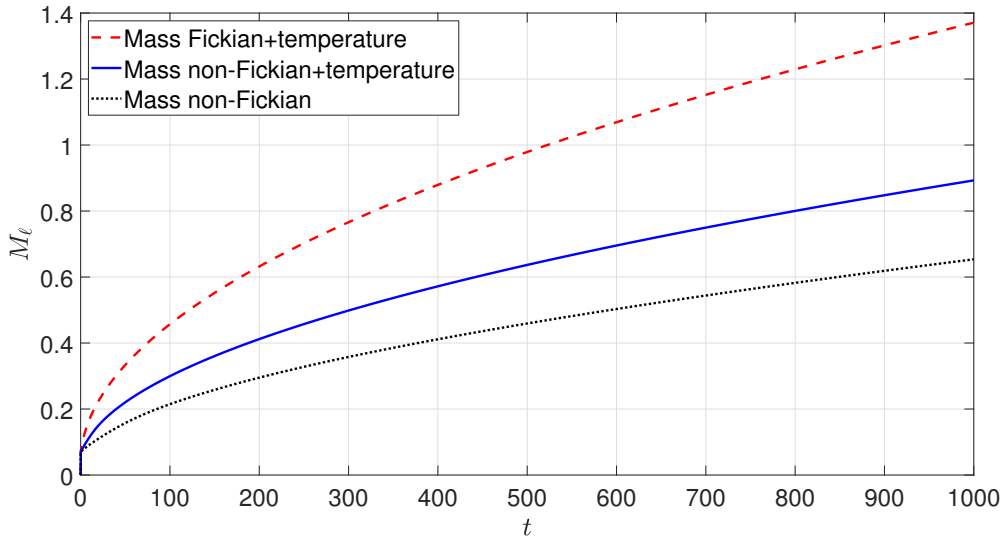

Figure 6: Mass variation of c_ℓ.

The plots in Figure 6 suggest the importance of including in the model the viscoelastic properties of the platforms, when analyzing the absorption of a permeant fluid. Moreover they

show that the opposition to fluid permeation, caused by the stress field, can be compensated by the effect of temperature.

To solve numerically the drug delivery problem (29)-(33), for c_d, we propose the following IMEX finite difference method

$$\begin{aligned} D_{-t}c^n_{d,h}(x_j) &= D_x^{\frac{1}{2}}(D_d(M_hT^n_h(x_j), M_hc^n_{\ell,h}(x_j))D_{-x}c^n_{d,h}(x_j)) \\ &+ D_x^{\frac{1}{2}}(D_v(M_hT^n_h(x_j), M_hc^n_{\ell,h}(x_j))\frac{M_hc^n_{d,h}(x_j)}{M_hc^n_{\ell,h}(x_j)}D_{-x}\sigma_h(T^n_h(x_j), c^n_{\ell,h}(x_j))) \\ &+ K_dc^n_{\ell,h}(x_j)\left(1-\frac{c^{n-1}_{d,h}(x_j)}{C_s(T^n_h(x_j))}\right)H(c^{n-1}_{s,h}(x_j))H\left(1-\frac{c^{n-1}_{d,h}(x_j)}{C_s(T^n_h(x_j))}\right), \end{aligned} \tag{36}$$

where σ_h is the non-Fickian part of the flux obtained from (35). As illustrated in Section 5.1, the numerical scheme (36) is second order convergent in space and first order convergent in time.

For c_s we consider

$$D_{-t}c^n_{s,h}(x_j) = -K_dc^n_{\ell,h}\left(1-\frac{c^n_{d,h}(x_j)}{C_s(T^n_h(x_j))}\right)(x_j)H(c^{n-1}_{s,h}(x_j))H\left(1-\frac{c^n_{d,h}(x_j)}{C_s(T^n_h(x_j))}\right). \tag{37}$$

The behavior of the concentration of dissolved drug c_d at $t = 0$, $t = 5 \cdot 10^2$ and $t = 10^3$ is plotted in Figure 7. We observe that as time increases, the amount of dissolved drug inside the domain also increases. A perfect sink condition is defined at $x = L$.

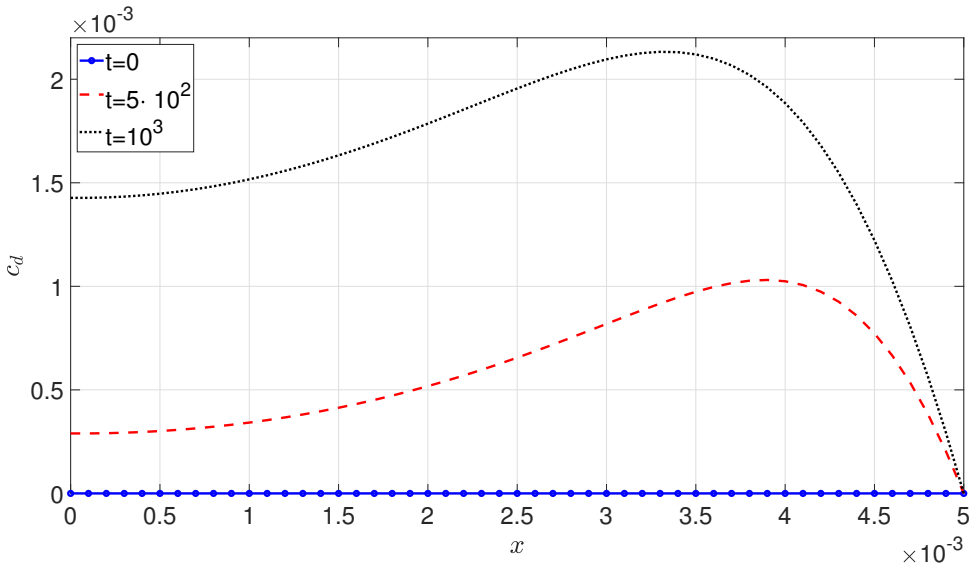

Figure 7: Concentration c_d for $t = 0$, $t = 5 \cdot 10^2$ and $t = 10^3$ in $[0, L]$.

In Figure 8 we show the concentration of dissolved drug c_d, at $t = t_f$ for the different regimes. We observe that the amount of dissolved drug is higher when the desorption is controlled by Fickian diffusion with a temperature enhancement. For the non-Fickian regime with no temperature enhancement, the concentration of dissolved drug c_d is smaller.

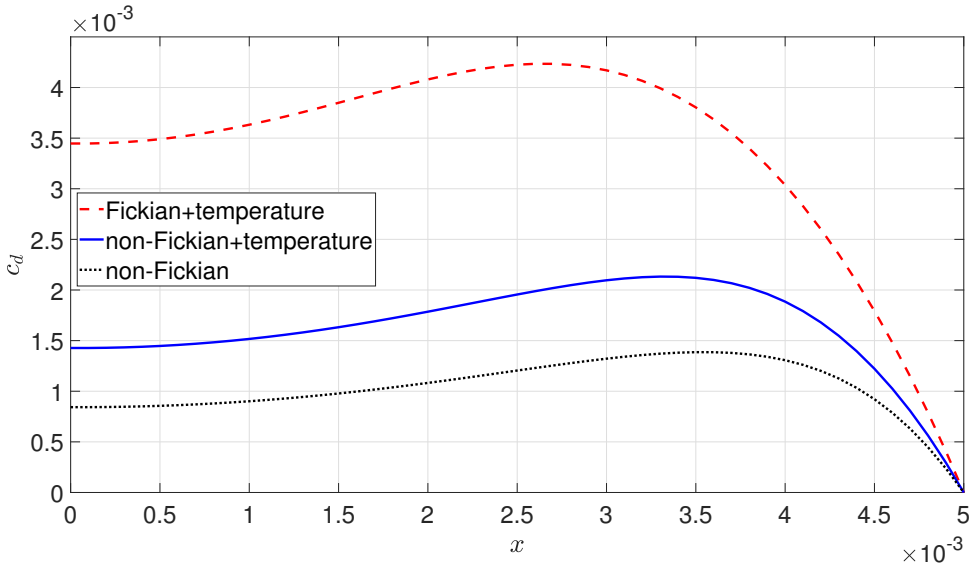

Figure 8: Concentration c_d for $t = t_f$ in $[0, L]$.

The mass of dissolved drug M_d is illustrated in Figure 9. In agreement with Figure 8, in the Fickian regime more fluid diffuses in the material, therefore the mass is higher. The amount of fluid in the non-Fickian regime is lower when compared with the other two regimes.

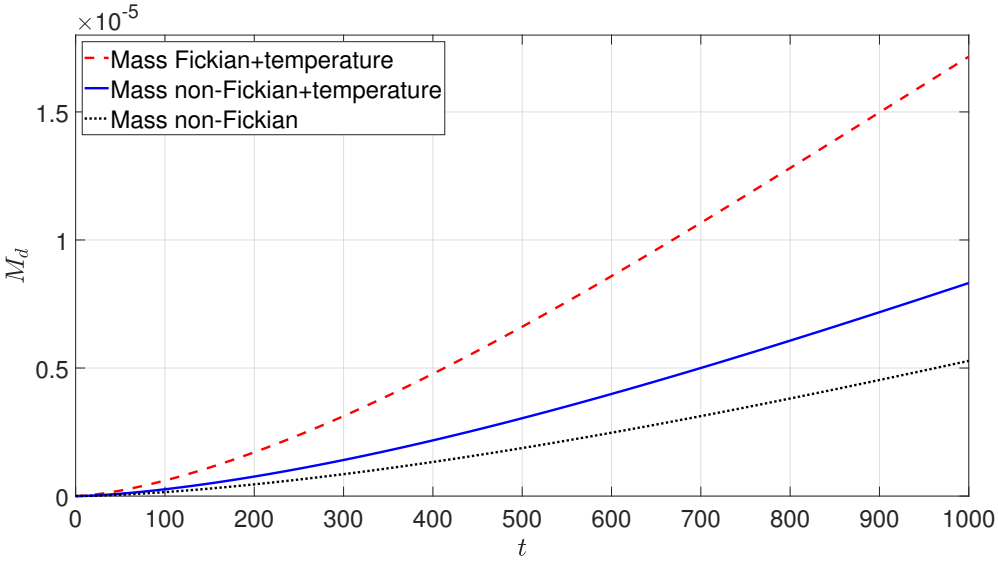

Figure 9: Mass M_d for $t = t_f$ in $[0, L]$.

The behavior of the concentration of solid drug c_s at $t = t_f$ is plotted in Figure 10. In this case, we notice a slowest dissolution when the entrance of fluid is not enhanced by the temperature. This outcome is consistent with the fact that if the amount of fluid in the system is smaller and the solubility does not increases with temperature, a greater amount of solid drug remains undissolved.

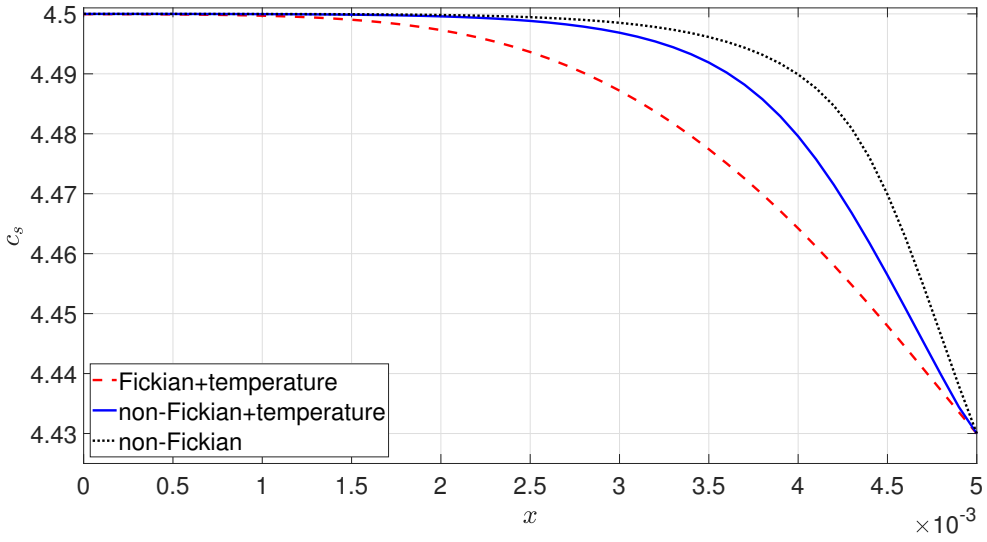

Figure 10: Concentration c_s for $t = t_f$ in $[0, L]$.

In order to illustrate the effect of the temperature as a drug release enhancer, we consider that a heat source is applied at the boundary of the domain. We assume the boundary condition $T(L,t) = 310 + 1 \times 10^{-3}t$ and set $t_f = 10^4$.

The behavior of the temperature is plotted in Figure 11. We can see that the temperature increases as t increases. The heat source is located at $x = L$.

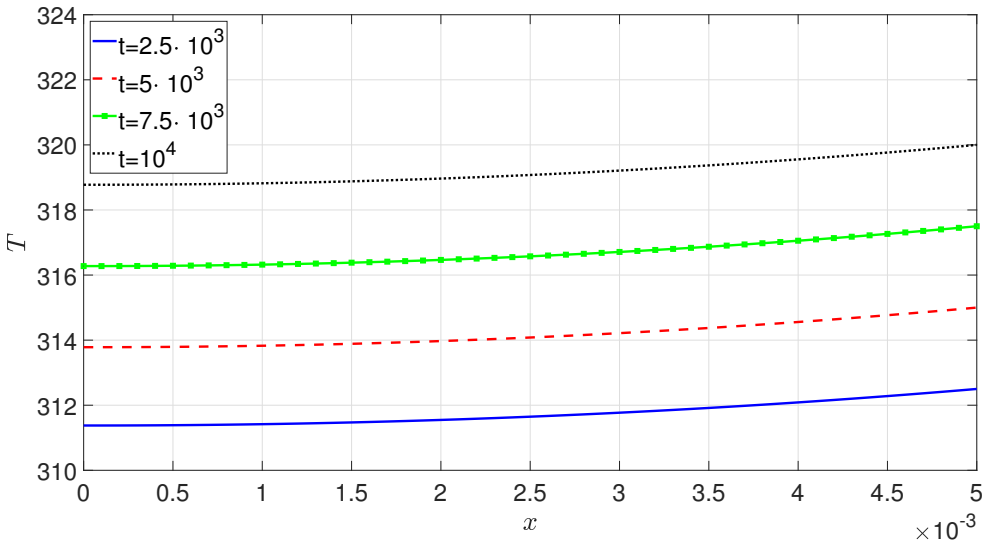

Figure 11: Temperature for $t = 2.5 \cdot 10^3$, $t = 5 \cdot 10^3$, $t = 7.5 \cdot 10^3$ and $t = 10^4$ in $[0, L]$.

In Figure 12 we study the effect of the heat source applied at the boundary for the concentration of fluid c_ℓ when the non-Fickiam model is used. We observe that as the temperature increases, the relaxation of the polymer is faster. Thus, the fluid diffuses faster in the material.

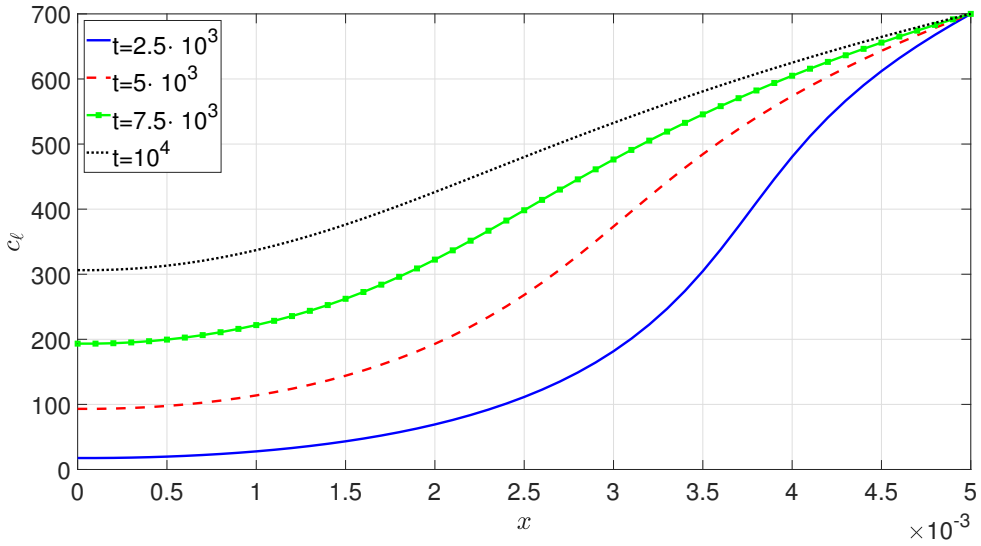

Figure 12: Concentration c_ℓ, computed with the non-Fickian model, for $t = 2.5 \cdot 10^3$, $t = 5 \cdot 10^3$, $t = 7.5 \cdot 10^3$ and $t = 10^4$ in $[0, L]$.

The increase of the temperature leads to an increase of the diffusion of c_ℓ. Since the dissolution of the drug is faster when more fluid is present and temperature is higher, we expect a faster drug delivery. This behavior is illustrated in Figure 13 for the concentration c_d of dissolved drug. We observe that in fact the heat induces an increase on c_d as time increases.

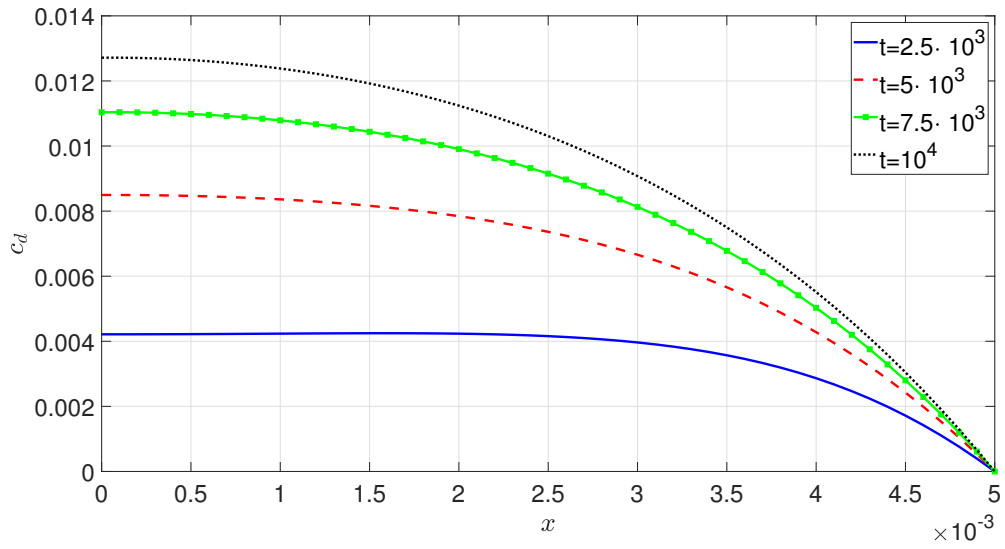

Figure 13: Concentration c_d, computed with the non-Fickian model, for $t = 2.5 \cdot 10^3$, $t = 5 \cdot 10^3$, $t = 7.5 \cdot 10^3$ and $t = 10^4$ in $[0, L]$.

5.1 Convergence rates

In what follows we illustrate the convergence orders in time and space for the numerical schemes proposed in Section 5.

In $\mathbb{W}_{h,0}$ we consider the inner product

$$(u_h, v_h)_h = \sum_{i=1}^{N-1} h_{i+1/2} u_h(x_i) v_h(x_i),$$

and denote by $\|\cdot\|_h$ the norm induced by this inner product.

For the numerical order in space, we consider an uniform partition $I_{\Delta t}$ of $[0,1]$, with $\Delta t = 1 \times 10^{-3}$. Assuming an initial uniform partition I_h for $[0, L]$, we compare the approximations T_h, $c_{\ell,h}$ and $c_{s,h}$, where h is halved successively. Hence, we define the errors by

$$\|E(u)\|_h = \max_{1 \leq n \leq M} \|u_h(t_n) - u_{\frac{h}{2}}(t_n)\|_h,$$

and the convergence rates

$$R_u = \log_2 \left(\frac{\|E(u)\|_h}{\|E(u)\|_{\frac{h}{2}}} \right).$$

In Table 1, we showcase the errors and the convergence orders in space for T_h, $c_{\ell,h}$ and $c_{d,h}$, considering the numerical schemes (34), (35) and (36), respectively. We observe that all the approximations are of quadratic order in space.

Table 1: Numerical order of convergence in space for T_h, $c_{\ell,h}$ and $c_{d,h}$.

h	$\|E(T)\|_h$	R_T	$\|E(c_\ell)\|_h$	R_{c_ℓ}	$\|E(c_d)\|_h$	R_{c_d}
$L/200$	4.80×10^{-4}	-	6.34×10^{-2}	-	5.43×10^{-12}	-
$L/400$	1.20×10^{-4}	1.9930	1.64×10^{-2}	1.9439	1.47×10^{-12}	1.8773
$L/800$	3.01×10^{-5}	1.9983	4.16×10^{-3}	1.9861	3.77×10^{-13}	1.9695
$L/1600$	7.55×10^{-6}	1.9996	1.04×10^{-3}	1.9965	9.50×10^{-14}	1.9908
$L/3200$	1.88×10^{-6}	1.9999	2.60×10^{-4}	1.9991	2.39×10^{-14}	1.9912

For the approximation of the convergence rates in time, we assume an uniform partition I_h of $[0, L]$ with $h = 1 \times 10^{-4}$. Considering an initial uniform partition $I_{\Delta t}$ for $[0,1]$, we compare the approximations $T_{\Delta t}$, $c_{\ell,\Delta t}$ and $c_{s,\Delta t}$, where Δt is halved successively. In this case, we define the errors by

$$\|E(u)\|_{\Delta t} = \max_{1 \leq n \leq M_{\Delta t}} \|u_{\Delta t}(t_n) - u_{\frac{\Delta t}{2}}(t_n)\|_h,$$

and the convergence orders

$$\hat{R}_u = \log_2 \left(\frac{\|E(u)\|_{\Delta t}}{\|E(u)\|_{\frac{\Delta t}{2}}} \right).$$

As we can observe in Table 2, all the approximations have linear order in time.

Table 2: Convergence rates in time for $T_{\Delta t}$, $c_{\ell,\Delta t}$ and $c_{s,\Delta t}$.

Δt	$\|E(T)\|_{\Delta t}$	$\hat{R}_T$	$\|E(c_\ell)\|_{\Delta t}$	$\hat{R}_{c_\ell}$	$\|E(c_d)\|_{\Delta t}$	$\hat{R}_{c_d}$
$t_f/6400$	5.27×10^{-3}	-	1.04×10^{-1}	-	6.59×10^{-11}	-
$t_f/12800$	2.85×10^{-3}	0.8845	5.32×10^{-2}	0.9710	3.31×10^{-11}	0.9941
$t_f/25600$	1.49×10^{-3}	0.9352	2.69×10^{-2}	0.9856	1.65×10^{-11}	0.9971
$t_f/51200$	7.64×10^{-4}	0.9666	1.35×10^{-2}	0.9928	8.30×10^{-12}	0.9986
$t_f/102400$	3.86×10^{-4}	0.9828	6.77×10^{-3}	0.9964	4.15×10^{-12}	0.9993

6 Conclusions

Controlled drug delivery devices that are enhanced by temperature can play an important role in the treatment of various diseases by allowing a targeted delivery of therapeutic agents to specific areas of the body. This minimizes the risk of side effects and maximizes the effectiveness of the treatment.

In this work we propose a novel mathematical model to describe non-Fickian absorption of a fluid into a polymeric matrix, followed by non-Fickian drug desorption, where both phenomena are enhanced by temperature. In the framework of Controlled Drug Delivery the permeating fluid represents the extracellular fluid. We deduce functional expressions depending on temperature/concentration for the viscoelastic diffusion coefficient and for the Young modulus of the springs considered in the mechanistic model.

It is shown that the diffusion problem is stable in bounded time intervals, provided that the functions T and c_ℓ are regular enough, and if the perturbation of the initial data for the temperature is bounded by an expression that depends on the physical parameters of the polymer. This restriction guarantees, from the mathematical point of view, that the parabolic part of equation (7) dominates the hyperbolic part. From the physical point of view the restriction ensures that the total flux is diffusion dominated and positive.

By coupling fluid absorption with drug delivery, we illustrate numerically two main aspects of the coupled phenomena: (i) the effectiveness of using heat to enhance drug release; (ii) the oversized predictions of the amount of delivered drug if viscoelastic properties are not considered. In fact, we observed that the relaxation of the polymer is increased when heat is considered leading to a faster absorption of the fluid and a subsequent enhancement of the release of the drug.

It is known that an increase in temperature in living tissue can cause an increase of drug permeation through the tissue. Therefore, the proposed model can be coupled with an external media in order to provide a realistic description of medical devices that can be used in the treatment of a wide range of diseases, from cancer to chronic pain.

Acknowledgments

Elías Gudiño was supported by Conselho Nacional de Desenvolvimento Científico e Tecnológico (CNPq), funded by the Brazilian Government trough the Ministério da Educação, grant 408215/2018-6.

José A. Ferreira and Paula de Oliveira were partially supported by Centro de Matemática da Universidade de Coimbra UID/MAT/00324/2013, funded by the Portuguese Government through FCT/MCTES and co-funded by the European Regional Development Fund through the Partnership Agreement PT2020.

References

[1] D. Liu, F. Yang, F. Xiong, N. Gu, The smart drug delivery system and its clinical potential, Theranostics 6 (9) (2016) 1306–1323.

[2] D. Rosenblum, N. Joshi, W. Tao, J. M. Karp, D. Pee, Progress and challenges towards targeted delivery of cancer therapeutics, Nature Commun. 9 (2018) 1410.

[3] L. Valdivia, L. García-Hevia, M. Bañobre-López, J. Gallo, R. Valiente, M. L. Fanarraga, Solid lipid particles for lung metastasis treatment, Pharmaceutics 13 (1) (2021) 93.

[4] A. Kumari, S. K. Yadav, S. C. Yadav, Biodegradable polymeric nanoparticles based drug delivery systems, Colloids Surf. B 75 (2010) 1–18.

[5] E. Blanco, M. Ferrari, Principles of nanoparticle design for overcoming biological barriers to drug delivery, Nat. Biotechnol. 33 (2015) 941–951.

[6] Y. Zhao, X. Fan, D. Liu, Z. Wang, Pegylated thermo-sensitive poly (amidoamine) dendritic drug delivery systems, Int. J. Pharm. 409 (2011) 229–36.

[7] G. Grassi, R. Farra, P. Caliceti, G. Guarnieri, S. Salmaso, M. Carenza, M. Grassi, Temperature-sensitive hydrogels, Am. J. Drug Deliv. 3 (2005) 239–251.

[8] J. A. Ferreira, P. de Oliveira, E. Silveira, Drug release enhanced by temperature: An accurate discrete model for solutions in h^3, Comput. Math. with Appl. 79 (2020) 852–875.

[9] J. A. Ferreira, P. de Oliveira, G.Pena, E. Silveira, Coupling nonlinear electric fields and temperature to enhance drug transport: An accurate numerical tool, J. Comput. Appl. Math. 384 (2021) 113127.

[10] L. N. Thomas, A. H. Windle, A deformation model for case ii diffusion, Polymer 21 (1980) 613–619.

[11] G. Camera-Roda, G. C. Sarti, Mass transport with relaxation in polymers, AIChE J. 36 (6) (1990) 851–860.

[12] D. S. Cohen, A. B. W. Jr., Sharp fronts due to diffusion and viscoelastic relaxation in polymers, SIAM J. Appl. Math. 51 (2) (1991) 472–483.

[13] M. Grassi, G. Grassi, Mathematical modeling and controlled drug delivery: Matrix systems, Curr. Drug Deliv. 2 (1) (2005) 97–116.

[14] J. A. Ferreira, M. Grassi, E. Gudiño, P. de Oliveira, A new look to non-Fickian diffusion, Appl. Math. Model. 39 (1) (2015) 194–204.

[15] H. F. Brinson, L. C. Brinson, Polymer Engineering Science and Viscoelasticity, An Introduction, Springer, New York, 2008.

[16] J. A. Ferreira, M. Grassi, E. Gudiño, P. de Oliveira, A 3D model for mechanistic control of drug release, SIAM J. Appl. Math. 74 (3) (2014) 620–633.

[17] F. Civan, Porous Media Transport Phenomena, John Wiley & Sons, New Jersey, 2011.

[18] G. Chiarappa, A. Piccolo, I. Colombo, D. Hasa, et. al., Exploring the shape influence on melting temperature, enthalpy, and solubility of organic drug nanocrystals by a thermodynamic model, Cryst. Growth Des. 17 (2017) 4072–4083.

[19] G. Chiarappa, Drug nanocrystals in drug delivery and pharmacokinetics, Ph.D. thesis, University of Trieste (2017).